Journal of Molecular Graphics and Modelling 47 (2014) 1–7

Contents lists available at ScienceDirect

Journal of Molecular Graphics and Modelling

journal homepage: www.elsevier.com/locate/JMGM

Homology modeling and docking studies of BjGL, a novel (+) gamma-lactamase from *Bradyrhizobium japonicum*

Dawei Song [a], Shaozhou Zhu [a], Xingzhou Li [b], Guojun Zheng [a,*]

[a] State Key Laboratory of Chemical Resources Engineering, Beijing University of Chemical Technology, Beijing, People's Republic of China
[b] Beijing Institute of Pharmacology and Toxicology, Beijing, People's Republic of China

ARTICLE INFO

Article history:
Accepted 14 October 2013
Available online 24 October 2013

Keywords:
Homology modeling
(+) Gamma-lactamases
Molecular docking
BjGL
Enantioselective hydrolysis

ABSTRACT

(+) Gamma-lactamases are enantioselective hydrolysis enzymes that can be used to produce optically pure (−) gamma-lactam, an important pharmaceutical intermediate for the anti-AIDS drug Abacavir. In this study, homology modeling and molecular dynamic simulation studies of a 3D homology model of BjGL, a novel (+) gamma-lactamase from *Bradyrhizobium japonicum*, were constructed and refined. The specific substrate (+) gamma-lactam and its enantiomer (−) gamma-lactam which can not be hydrolyzed was docked into the active site respectively, and the catalytic triad and other crucial residues that participate in the formation of the hydrophobic binding pocket, hydrogen bonds, and the oxyanion hole were identified. Furthermore, possible reasons for the high diastereoselectivity of BjGL binding with the substrate are proposed.

1. Introduction

Amidase-catalyzed hydrolytic biotransformations are very important in the field of chiral drug synthesis due to their high enantioselectivity, mild reaction conditions, and low environmental impact [1–4]. The current known (+) gamma-lactamases [5,6] belong to the typical amidase superfamily (EC 3.5.1). When reacting with (rac) gamma-lactam 2-azabicyclo[2.2.1]hept-5-en-3-one, (+) gamma-lactamases can stereoselectively catalyze the introduction of one molecule of water into the specific substrate (+) gamma-lactam (+) 2-azabicyclo[2.2.1]hept-5-en-3-one, cleaving the amide bond to produce optically pure (−) gamma-lactam (−) 2-azabicyclo[2.2.1]hept-5-en-3-one, an important pharmaceutical intermediate in the synthesis of the anti-AIDS drug Abacavir [5,7].

Until now, only two (+) gamma-lactamases have been cloned, expressed, and purified. One is from *Sulfolobus solfataricus* and the other is from *Comamonas acidovorans*, and they are both used in the industrial production of (−) gamma-lactam [5,6,8–10]. The amino acid sequence of the (+) gamma-lactamase from *S. solfataricus* (*SSO*) shares about 40% identity with the amidases from *Rhodococcus rhodochrous* J1 and *Rhodococcus* sp. N-771. The amino acid sequence of the (+) gamma-lactamase from *C. acidovorans* is very similar to a formamidase from *Bradyrhizobium japonicum* USDA 6 and another formamidase from *Methylophilus methylotropus*. However, research has indicated that the two (+) gamma-lactamases from *S. solfataricus* and *C. acidovorans* share no identity, which means that two different kinds of amidases can show similar (+) gamma-lactamase activity [11]. Both of these (+) gamma-lactamases have been crystallized, but X-ray crystallography of the (+) gamma-lactamases has not yet been performed, perhaps due to the difficulty of the determination and refinement processes of the new crystal structures, or to the insufficient quality of the crystal structures themselves [12,13]. It is expected that a better understanding of the structural properties of these (+) gamma-lactamases will be beneficial to the study of molecular catalytic mechanisms.

Computational approaches can provide homology modeling, molecular dynamic simulations, and automatic docking in order to demonstrate the function of proteins and to illustrate the mode of substrate binding. These types of methods can be used successfully in enzyme–substrate systems and can provide useful information for future studies [14–16]. The main objective of the present work is to introduce a three-dimensional (3D) model of a novel (+) gamma-lactamase that was cloned from *B. japonicum* USDA 6 [11] and docked to the enantiomers (+/−) gamma-lactam, respectively, as well as to obtain information about the active site and residues. The information about the catalytic and binding domains of *B. japonicum* USDA 6 (+) gamma-lactamase (BjGL) is crucial to understanding both the substrate's mode of action and the catalytic mechanism. Because the function of an enzyme is determined by its structure, molecular modeling and docking studies can provide extensive structural details. The active site and binding pocket were identified, and the key residues involved in ligand binding were

* Corresponding author. Tel.: +86 1064437507.
E-mail address: zhenggj@mail.buct.edu.cn (G. Zheng).

1093-3263/$ – see front matter © 2013 Elsevier Inc. All rights reserved.
http://dx.doi.org/10.1016/j.jmgm.2013.10.006

also determined. Finally, through comparative analysis of interaction energy between ligands and enzyme, differences in hydrogen bonding interaction and the distances between ligands and crucial residues, the mechanism for BjGL highly stereoselective catalyzing (+) gamma-lactam hydrolyzation was proposed.

2. Methods

2.1. Homology modeling and energy minimization

The protein sequence of BjGL was downloaded from the NCBI protein sequence database with accession number YP_005605100 (http://www.ncbi.nlm.nih.gov/protein). In order to identify homologous sequences with known 3D structures and find related protein structures as templates, a protein–protein BLAST [17] was performed against the NCBI protein data bank (PDB) database using BjGL as a query sequence. According to the BLAST results, the template structure was downloaded from the RCSB Protein Date Bank [18] (http://www.rcsb.org/pdb/). The target sequence was then aligned to the template sequence using Discovery Studio 2.5 and the Align 123 program (Accelrys Software, Inc., San Diego, CA), and a gap open penalty of 10 and the BLOSUM30 scoring matrix were utilized. 10 homology models of BjGL were then generated by submitting the sequence alignments to the DS 2.5 homology model building program Modeler 9v4 [19]. The 3D models were ranked based on probability density function (PDF) total energy and evaluated by Verify Protein (Profiles-3D) [20] and Ramachandran plot [21]. According to these validation results, the best homology model was chosen for further refinement. Using the LOOPER program [22] as a regional energy minimization tool, four rounds of loop refinement were implemented on the loop regions with negative scores. The optimized 3D model of BjGL was verified by Verify Protein (Profiles-3D), PROCHECK [23], and ProSa-web [24].

The global energy minimization (EM) was carried out under CHARMm [25] force fields using DS 2.5 simulation protocols. The model of BjGL was solvated with an explicit periodic boundary solvation model. The orthorhombic water solvation model contained 0.145 mol/L sodium and chloride, and the minimum distance from the boundary was set to 7 Å to simulate the real catalytic reaction environment. A three-stage EM protocol was employed for the solvated enzyme energy minimization [26]. At each stage, minimization was executed with 3000 steps of the steepest descent algorithm and 6000 steps of the conjugate gradient algorithm, with minimization criteria set at 0.1 and 0.001 RMSG, respectively. In the first stage, the protein was constrained and only the solvation model was minimized. In the second stage, the heavy atoms were constrained and the hydrogen atoms of the protein were relaxed, and both the solvent molecules and the protein hydrogen atoms were minimized. In the third stage, all the solvation model molecules and protein atoms were allowed to relax. After the optimization procedure, the final 3D model of BjGL was chosen for further study.

2.2. Active site analysis

The active site was obtained and reconfirmed in three steps. In the first step, the potential binding site was predicted according to the model surface cavities using the DS 2.5 Analyze Binding Site tool; Because the BjGL model with template 3A1I and the *SSO* amidase shared considerable sequence identity and similar structural properties, the second step involved multiple sequence alignments of the BjGL with template 3A1I and the *SSO* amidase, comparisons and analyses of the active residues reported in previous research [8,27,28] were utilized to facilitate the identification of the model binding site; In the third step, after superposing the model structure with template 3A1I, the active site information was obtained by X-ray diffraction to reconfirm the potential active site. As a result, the predicted site was chosen as the most favorable binding site for docking with the substrate.

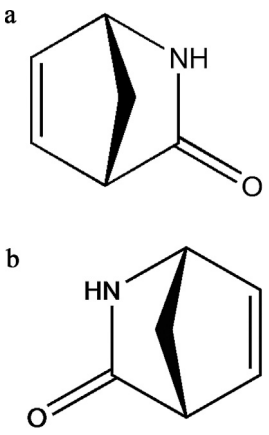

Fig. 1. Structure of the substrate (+) gamma-lactam and its chiral isomer (−) gamma-lactam.

2.3. Molecular dynamic simulation and docking study of modeled (+) gamma-lactamase

The 2D structure of (+) gamma-lactam and its chiral isomer (−) gamma-lactam was shown in Fig. 1. 3D structures of the chiral ligands were generated by the DS 2.5 Build Fragment tool through energy minimization optimized by the Prepare Ligands protocol in DS 2.5, and by adding CHARMm [25] force fields for docking.

The docking study was processed by CDOCKER [29], a CHARMm-based molecular dynamics (MD) method for ligand docking in DS 2.5. In the beginning high-temperature MD simulation, 20 random conformations for each chiral ligand were generated by 5000 steps at a target temperature of 1000 K. The grid extension was set to 4 Å. 20 random orientations of each ligand conformation were generated. These conformations were then translated into receptors and moved into the binding sphere. As soon as each ligand conformation was docked into the protein active site, an MD simulation was carried out, with a gradual heating phase of a 2000 steps, 1 fs per step, from 300 to 700 K, followed by a cooling phase of 5000 steps, 1 fs per step, returning back down to 300 K [15]. A final full potential minimization was then used to refine the ligand poses. According to the CDOCKER scores, the best-docked conformation of the substrate (+) gamma-lactam and its chiral isomer (−) gamma-lactam was retrieved for post-docking analysis.

3. Results

3.1. Homology modeling and EM

Protein–protein BLAST searches for BjGL resulted in a large number of sequences. Through sequence similarity analysis, the results implied that BjGL belongs to the amidase superfamily (PRK07235). Further high-similarity multiple sequence alignments of BjGL revealed a resemblance to *R. rhodochrous* amidase 3A1K and *SSO* amidase, as shown in Fig. 2. The target sequence showed 43.6% identity and 64.0% similarity with the sequence of *R. rhodochrous* amidase [27] (PDB codes: 3A1K and 3A1I). The crystal structures of *R. rhodochrous* amidase (PDB code: 3A1K) and its enzyme–substrate complex with benzamide (PDB code: 3A1I) at resolutions of 2.17 Å and 2.32 Å, respectively, were chosen as templates for the homology modeling. The crystal structure of *R. rhodochrous* amidase complexed with the substrate benzamide

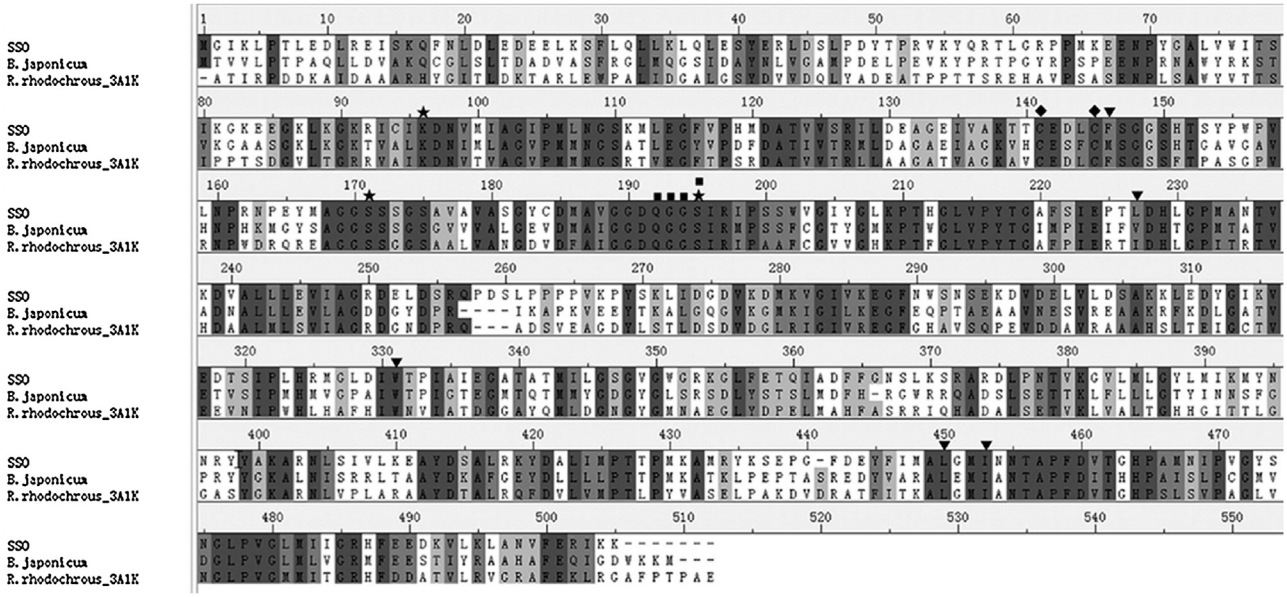

Fig. 2. Multiple sequence alignments of the target sequence (*B. japonicum* USDA 6 (+) gamma-lactamase) with the template sequence (*R. rhodochrous* amidase) and the (+) gamma-lactamase from *S. solfataricus* (*SSO*). Notes: The highly conserved catalytic triad residues are marked with a pentagram; the Cys-X_3-Cys motif is marked with a rhombus; the residues constituting the oxyanion hole are marked with a square; and the conserved hydrophobic residues are marked with an inverted triangle.

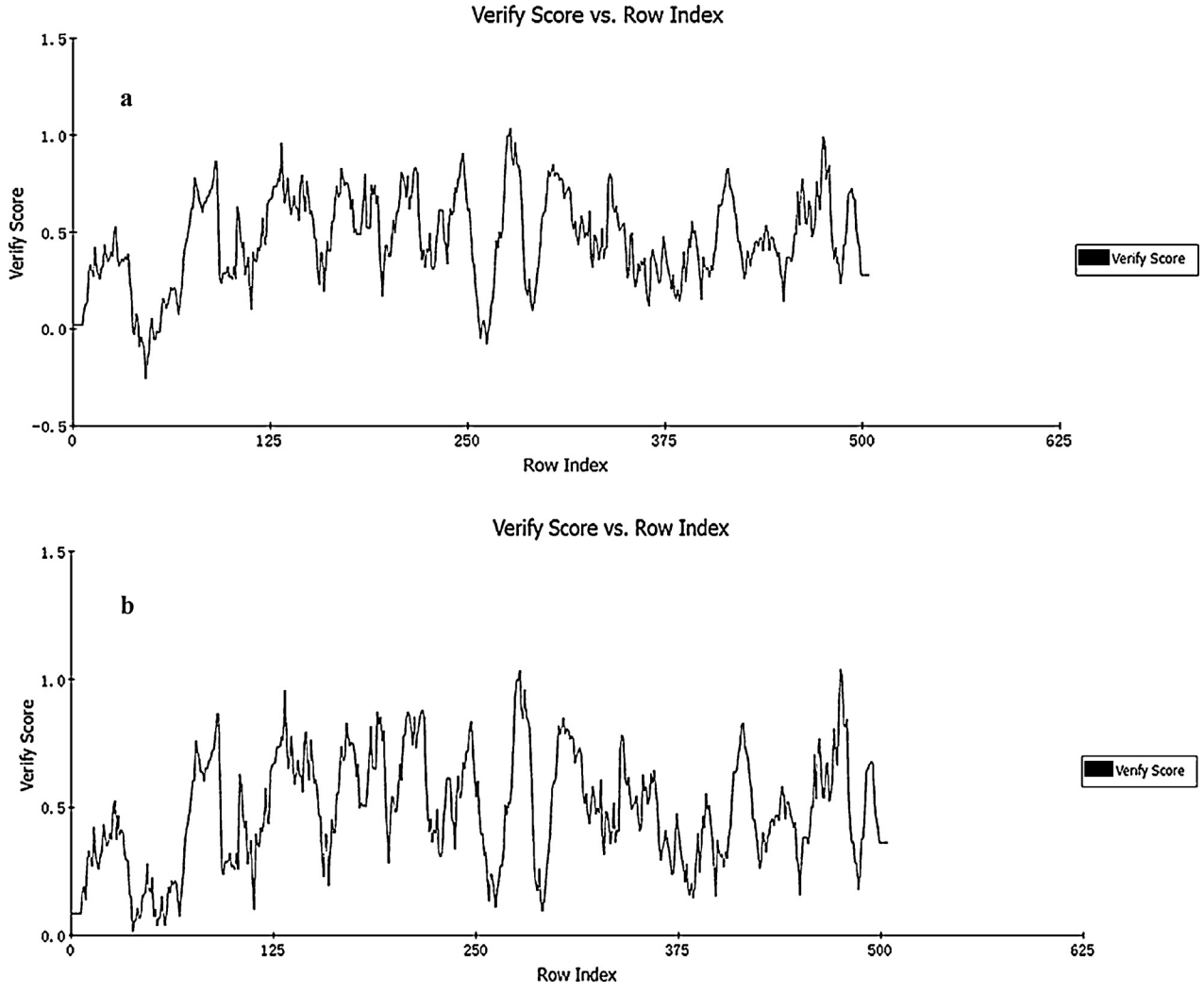

Fig. 3. Profiles-3D line plot of BjGL: (a) initial model and (b) model after loop refinement. Notes: residues with negative verify scores are unreasonably folded.

Table 1
Protein structure analysis of the initial model and the optimized model.

Model	Initial	Optimized
Verify-3D[a]	95.44	100
Profiles-3D[b]	208.33	219.71
Potential energy (kcal/mol)	134839.05	−20214.39
van der Waals energy (kcal/mol)	146161.90	−3994.76
Electrostatic energy (kcal/mol)	−16331.66	−18383.06

[a] Percentage of total residues with averaged 3D–1D score > 0;
[b] The minimum and maximum possible scores for the BjGL model are 103.632 and 230.294, respectively.

has a structural similarity with the known specific substrate (+) gamma-lactam of (+) gamma-lactamase. This increased our confidence in using these crystal structures (PDB codes: 3A1I and 3A1K) for the homology modeling of BjGL, and further molecular docking was utilized to identify the active binding site residues.

The 3D molecular models were generated by Modeler 9v4 in DS 2.5. Building the homology models involved performing a high level of molecular dynamics with simulated annealing and loop refinement on detected loop regions (model sequence segments that are not aligned with the templates) of at least 5 residues to acquire high-quality initial model structures. Based on PDF total energy, Verify Protein (Profiles-3D) score, and Ramachandran plot, the best model was chosen from 10 initial models for further refinement. Using Verify Protein (Profiles-3D) to calculate the compatibility score of each residue, two loop regions were detected in the negative score region: ASP39-LYS55 and LYS258-GLU263 (Fig. 3a). In conjunction with the two defective loop regions, 4 rounds of loop refinement were performed. After the optimization, the refined model received a verify score of 219.71 (Table 1), which is close to the expected high score of 230.294, and the two loop regions were in the reasonable area (Fig. 3b). The final model was validated using PROCHECK and ProSa-web. The Ramachandran plot shows that the backbone dihedral angle distribution of all the amino acid residues is as follows: 90.3% were in the most favored regions, 9.2% were in additional allowed regions, and 0.2% were in generously allowed regions (Fig. 4). Further analysis suggests the three residues (Pro260, Pro391 and Asp500) which are located in disallowed region are far from enzyme's active site. This indicates that

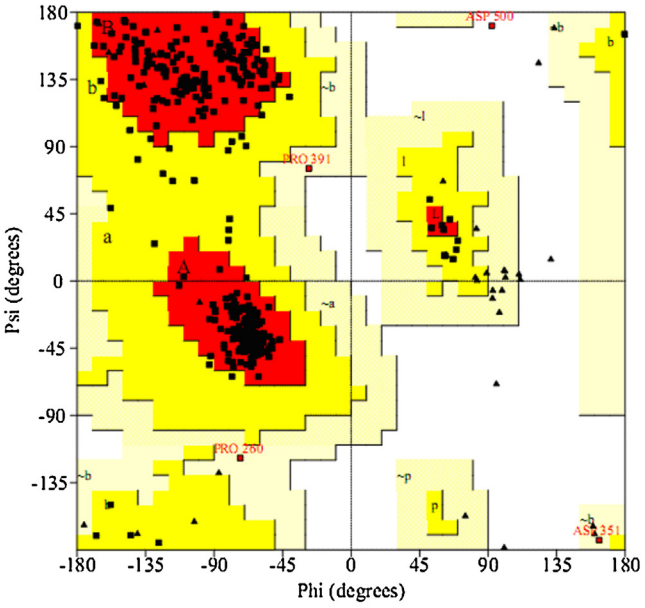

Fig. 4. Ramachandran plot of *B. japonicum* USDA 6 (+) gamma-lactamase obtained by PROCHECK.

Fig. 5. Final 3D structure of *B. japonicum* USDA 6 (+) gamma-lactamase. Notes: The α-helix is represented by red, the β-sheet is shown in blue, the β-turn is represented by green, and the random coil is illustrated in light gray.

the backbone dihedral angles psi and phi in the BjGL model were reasonably accurate. The ProSa *z*-score was −8.18, which is within the range of scores typically found for native proteins of similar size. The model was also evaluated by superimposing it onto the template crystal structure; the RMSD was 1.775 Å based on the main chain atoms. Taken together, these evaluation results reveal that the optimized model is satisfactory and can be considered to be a reliable source for the rest of the study.

The global energy minimization of the optimized model was continued using the EM methods mentioned in Section 2.1. During the three-stage gradual EM procedure, the aim of the first step was to remove the bad contacts among solvent molecules. The aim of the second step was to optimize the locations of the hydrogen atoms, which have an important influence on the geometry of the hydrogen bonds. A comparison of the energy variation of the initial and optimized models is shown in Table 1, and the final 3D predicted structure of BjGL is depicted in Fig. 5.

3.2. Active site analysis

Active site information was obtained by the method described in Section 2.2. The results of sequence similarity analyses and tertiary structure comparisons indicate that BjGL possesses the

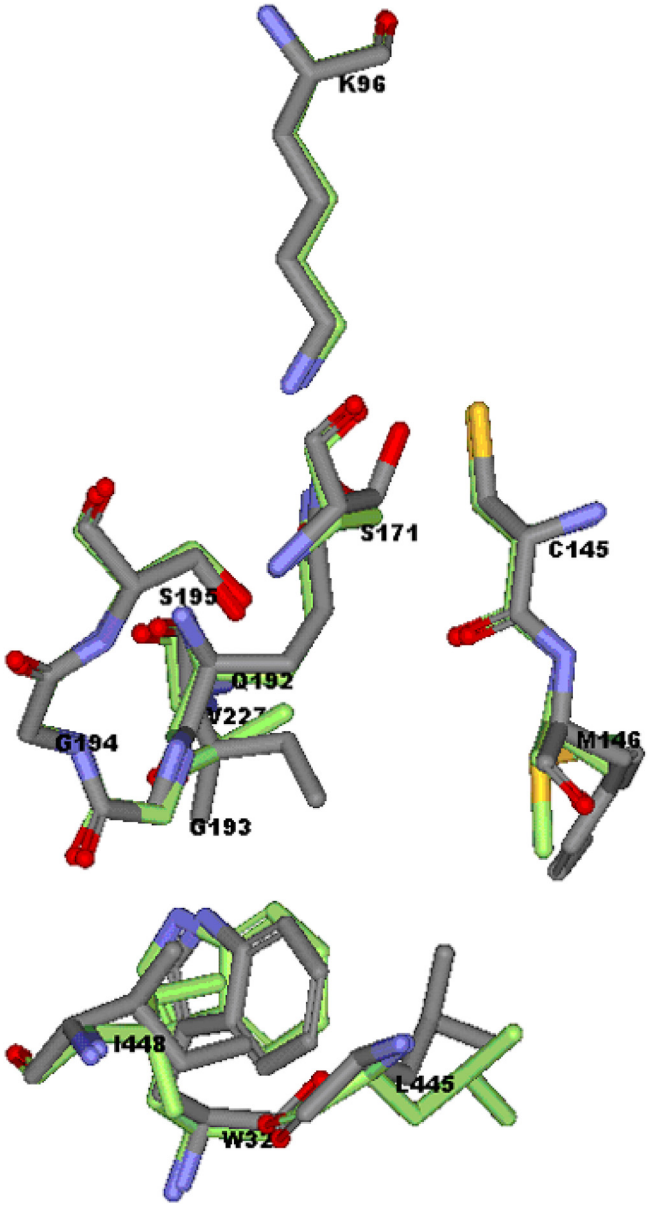

Fig. 6. Superimposition of active site residues of template 3A1I and *B. japonicum* USDA 6 (+) gamma-lactamase model. Notes: Gray and green residues represent the template and the homology model, respectively.

classical Ser-cisSer-Lys catalytic triad and a Cys-X_3-Cys motif [27,28], which are highly conserved in the amidase signature (AS) family. The active site of the modeled BjGL is located in the middle of the core structure. The catalytic triad is constituted by Ser171-Ser195-Lys96, which corresponds to the template structure (Figs. 2 and 6). The conserved hydrophobic pocket in the target protein is constituted by residues Met146, Val227, Trp327, Leu445, and Ile448. Compared with the template, only Met146 and Val227 are replaced by amino acids of the same group, i.e., Phe146 and Ile227 (Figs. 2 and 6). Moreover, the oxyanion hole, which closely relate to electron transfer during intermolecular hydrogen bonds formation, is constituted by Gln192, Gly193, Gly194, and Ser195 in the template protein is also found in the target protein, and the constituent residues are highly conserved (Figs. 2 and 6).

3.3. Docking study

In order to meet the requirements of the enzyme–substrate interaction (i.e., the fitted conformation of the substrate, suitable docking orientation to the enzyme, and the formation of the appropriate enzyme–substrate binding pose), CDOCKER was chosen as the docking method. According to the CDOCKER scores, the best docking pose (Fig. 7a) was screened out from 20 optimized docking poses. The interaction energy of the substrate with each of the residues around the binding pocket was calculated to assist the confirmation of the key residues that comprise the binding pocket of the model. The significant binding site residues in the model were then identified according to the total interaction energy between the ligand and each amino acid in the enzyme. This identification, in contrast to a definition based on the distance from the ligand, can clearly illustrate the relative significance for every residue. As a control group, the enantiomer (−) gamma-lactam was also docked into the active site with the same method (Fig. 7b). (−) Gamma-lactam-BjGL docking result was analyzed using the same analytical methods (i.e., the hydrogen bond formation, the interaction energies, and distances between crucial residues and ligand).

3.4. Analyzing of BjGL substrate diastereoselectivity

Table 2 lists the comparison of different types of interaction energy, Including van der Waals, electrostatic and total interaction energy. Obviously, the (+) gamma-lactam-BjGL complex has a favorable total interaction energy and electrostatic energy. The total interaction energy required for docking (+) gamma-lactam to BjGL is half of the energy for docking (−) gamma-lactam, while the electrostatic energy required for docking the (+) enantiomer is one-third of the (−) enantiomer. This makes (−) gamma-lactam at a disadvantage in the competition of binding with BjGL active site. The low interaction energy of (+) gamma-lactam-BjGL also indicates that (+) gamma-lactam has a strong interaction with BjGL. And the strong interaction is much more conductive to (+) gamma-lactam hydrolyzation which is catalyzed by BjGL.

It is well known that hydrogen bonds play a significant role in substrate orientation and enzyme–substrate intermediate complex formation [30]. There are two important hydrogen bonds between (+) gamma-lactam and BjGL. A hydrogen bond of 1.88 Å was observed between the hydroxyl group of Ser195 and the O8 of (+) gamma-lactam. The other hydrogen bond of 2.06 Å was formed by the carboxylate oxygen of Cys145 with the N6 of (+) gamma-lactam. These two amino acid residues help to form hydrogen bonds and are located in the two corners of the active pocket (Fig. 7a).

Table 2
Total energy (E_{total}), van der Waals energy (E_{vdw}), and electrostatic energy (E_{ele}) of individual residues of BjGL and (+/−) gamma-lactam.

Residues	(+) Gamma lactam			(−) Gamma lactam		
	E_{total}	E_{vdw}	E_{ele}	E_{total}	E_{vdw}	E_{ele}
Total	−39.61	−10.91	−28.7	−18.15	−9.48	−8.57
LYS 96	−4.07	−0.03	−4.04	−6.46	−0.04	−6.41
CYS 145	−3.44	−0.82	−2.62	1.24	−1.04	2.28
MET 146	−2.13	−2.40	−0.27	−1.63	−1.58	−0.05
SER 171	−2.82	−0.91	−1.91	−4.02	−0.77	−3.25
GLY 190	−0.91	−0.04	−0.87	−1.56	−0.05	−1.51
GLN192	−0.64	−0.72	−0.09	−0.49	−0.82	0.33
GLY 193	−1.13	−0.75	−0.38	0.33	0.25	0.08
GLY 194	−1.42	−0.61	−0.81	−0.74	−0.66	−0.08
SER 195	−6.27	−1.05	−5.23	−3.96	−1.66	−2.30
ARG 197	−7.32	−0.04	−7.28	0.33	−0.05	0.38
TRP 327	−1.69	−1.05	−0.64	−1.67	−0.99	−0.68
LEU 445	−0.94	−0.95	0.01	−0.90	−0.76	−0.15
GLU 446	−5.49	−0.05	−5.45	2.56	−0.04	2.60
ILE 448	−1.35	−1.50	0.16	−1.19	−1.37	0.18

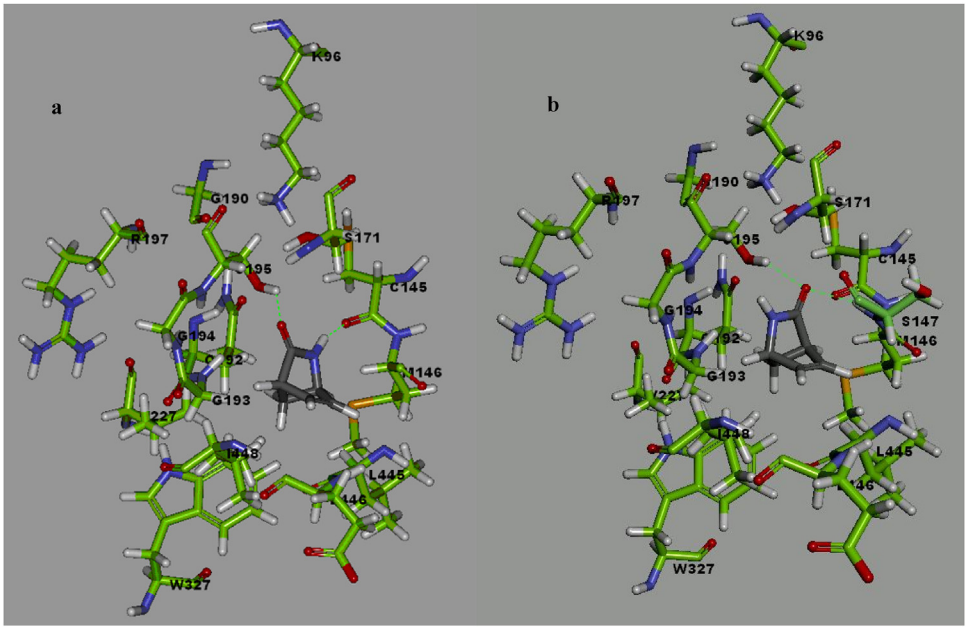

Fig. 7. (a) Binding model of (+) gamma-lactam in the active site of *B. japonicum* USDA 6 (+) gamma-lactamase; (b) binding model of (−) gamma-lactam in the active site of *B. japonicum* USDA 6 (+) gamma-lactamase. Notes: Residues of *B. japonicum* USDA 6 (+) gamma-lactamase, which participate in interactions with the ligand (shown in gray), are shown in green, and H-bonds are shown as green dotted lines.

When hydrogen bonds are formed with the substrate, an electron donor (Ser195) and an electron accepter (Cys145) are matched with the electrical properties of the substrate. While in control group, (−) gamma-lactam – BjGL docking result (Fig. 7b) indicates that Ser147 and Ser195 formed a hydrogen bond with O8 of (−) gamma-lactam, respectively, meanwhile the imino group of (−) gamma-lactam remained in a free state. This way of interaction may lead to improper orientation of (−) gamma-lactam in BjGL active site and weaken the combination between ligand and enzyme.

Further more, through comparing the distances between residues which relate to hydrogen bond formation and active group of chiral ligands (Fig. 8), it was found that the lengths of hydrogen bonds between (+) gamma-lactam and BjGL are ~2 Å. And the distances between O8 of (+) gamma-lactam and Gly193 Gly194, which comprise the oxyanion hole and participating catalyzing lactam bond hydrolyzation, are within 5 Å. While in (−) gamma-lactam-BjGL docking result, the distances between carbonyl group and imino group of (−) gamma-lactam and hydrogen bond participant (Ser195, Cys145) are all farther than (+) gamma-lactam-BjGL's. In addition, because of the difference in stereo configuration and mirrored orientation in active site, the distances between (−) gamma-lactam carbonyl group and Gly 193 Gly194 are also farther than that of (+) gamma-lactam-BjGL.

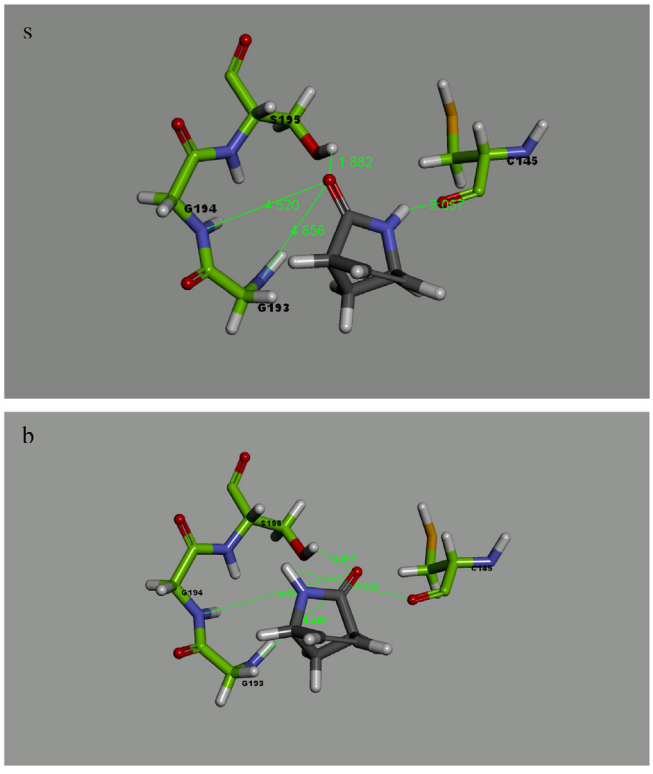

Fig. 8. Comparing of distances between crucial residue of (+) gamma-lactamase and (+/−) gamma-lactam. Notes: (a) (+) gamma-lactam in (+) gamma-lactamase; (b) (−) gamma-lactam in (+) gamma-lactamase.

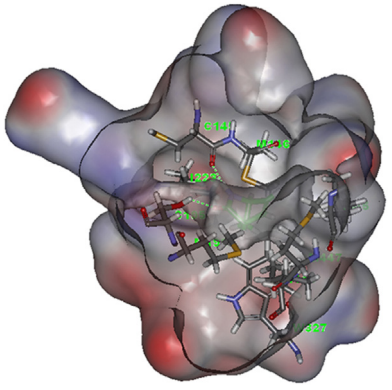

Fig. 9. (+) Gamma-lactam in (+) gamma-lactamase and interacted with hydrophobic pocket. Notes: Binding site hydrophobic residues are illustrated as gray sticks, the formed hydrophobic pocket is shown as a gray semitransparent membrane, the ligand is symbolized by green sticks, and H-bonds are represented as green dotted lines.

Meanwhile, the shape of the enzyme binding pocket strongly influences the catalytic selectivity of the substrate, especially the enzyme's ability to selectively catalyze chiral compounds. Interaction studies also showed the presence of a hydrophobic pocket in the binding pocket formed by residues Met146, Met198, Ile223, Trp327, Leu445, Met447, and Ile448. These amino acid residues formed a boat-shaped hydrophobic pocket (Fig. 9). This pocket was well matched with the stereoscopic configuration of (+) gamma-lactam and was occupied by the hydrophobic part of the substrate (i.e., cyclopentenyl in the case of (+) gamma-lactam), as depicted in Fig. 9. The fact that the substrate's stereoscopic configuration corresponds to the shape of the binding pocket contributes to BjGL specifically recognizing and combining only one configuration (i.e., (+) gamma-lactam) of (rac) gamma-lactam.

4. Conclusions

To our knowledge, this study represents the first reported structural analysis of BjGL based on a 3D structural model of the BjGL – (+) gamma-lactam complex using molecular simulation. The active site, binding pocket, and key residues involved in the catalytic event of BjGL were identified. Hopefully, this study will facilitate a better understanding of enzyme-substrated complex's mode of action and guide future rational design studies. The interactions between the enzyme and the substrate proposed in this study could help researchers better understand the potential mechanism of BjGL. Furthermore, it is expected that this approach will aid the identification of the mutation sites that influence enzyme activity. Ideally, the findings of this study will stimulate future biochemical investigations and guide the design of enzymes to improve the utilization of (rac) gamma-lactam for the production of valuable (−) gamma-lactam.

References

[1] A. Schmid, F. Hollmann, J.B. Park, B. Bühler, The use of enzymes in the chemical industry in Europe, Curr. Opin. Biotechnol. 13 (2002) 359–366.
[2] V. Vejvoda, L. Martínková, A.B. Veselá, O. Kaplan, S. Lutz-Wahl, L. Fischer, B. Uhnáková, Biotransformation of nitriles to hydroxamic acids via a nitrile hydratase-amidase cascade reaction, J. Mol. Catal. B: Enzymol. 71 (2011) 51–55.
[3] R. Wohlgemuth, Asymmetric biocatalysis with microbial enzymes and cells, Curr. Opin. Microbiol. 13 (2010) 283–292.
[4] R.N. Patel, Synthesis of chiral pharmaceutical intermediates by biocatalysis, Coord. Chem. Rev. 252 (2008) 659–701.
[5] S.J.C. Taylor, R.C. Brown, P.A. Keene, I.N. Taylor, Novel screening methods-the key to cloning commercially successful biocatalysts, Bioorgan. Med. Chem. 7 (1999) 2163–2168.
[6] H.S. Toogood, R.C. Brown, K. Line, P.A. Keene, S.J.C. Taylor, R. McCagueb, J.A. Littlechild, The use of a thermostable signature amidase in the resolution of the bicyclic synthon (rac)-γ-lactam, Tetrahedron 60 (2004) 711–716.
[7] S.J.C. Taylor, R. McCague, R. Wisdom, C. Lee, K. Dickson, G. Ruecroft, F. O'Brien, J. Littlechild, J. Bevan, S.M. Roberts, C.T. Evans, Development of the biocatalytic resolution of 2-azabicyclo[2.2.1]hept-5-en-3-one as an entry to single-enantiomer carbocyclic nucleosides, Tetrahedron: Asymmetr. 4 (1993) 1117–1128.
[8] E. Cilia, A. Fabbri, M. Uriani, G.G. Scialdone, S. Ammendola, The signature amidase from *Sulfolobus solfataricus* belongs to the CX3C subgroup of enzymes cleaving both amides and nitriles, FEBS J. 272 (2005) 4716–4724.
[9] K.E. Holt-Tiffin, (+) – and (−)-2-azabicyclo [2.2.1] hept-5-en-3-one: extremely useful synthons, Chim. Oggi. 27 (2009) 23–25.
[10] J. Wang, X. Zhang, C. Min, S. Wu, G. Zheng, Single-step purification and immobilization of γ-lactamase and on-column transformation of 2-azabicyclo [2.2.1] hept-5-en-3-one, Process. Biochem. 46 (2011) 81–87.
[11] S. Zhu, C. Gong, D. Song, S. Gao, G. Zheng, Discovery of a novel (+)-γ-lactamase from *Bradyrhizobium japonicum* USDA 6 by rational genome mining, Appl. Environ. Microbiol. 78 (2012) 7492–7495.
[12] V. Nastopoulos, B. Vallone, L. Politi, A.S. d'Abusco, R. Scandurra, D. Tsernoglou, Crystallization and X-ray diffraction measurements of a thermophilic archaeal recombinant amidase from *Sulfolobus solfataricus* MT4, Acta. Crystallogr. D: Biol. Crystallogr. 57 (2001) 1036–1037.
[13] I.S. Gonsalvez, M.N. Isupov, J.A. Littlechild, Crystallization and preliminary X-ray analysis of a γ-lactamase, Acta. Crystallogr. D: Biol. Crystallogr. 57 (2001) 284–286.
[14] X.Y. Meng, Q.C. Zheng, H.X. Zhang, A comparative analysis of binding sites between mouse CYP2C38 and CYP2C39 based on homology modeling, molecular dynamics simulation and docking studies, Biochim. Biophys. Acta 1794 (2009) 1066–1072.
[15] M. Tiwari, J.K. Lee, Molecular modeling studies of L-arabinitol 4-dehydrogenase of *Hypocrea jecorina*: its binding interactions with substrate and cofactor, J. Mol. Graph. Model. 28 (2010) 707–713.
[16] R. Kumar, S. Kumar, S. Sangwan, I.S. Yadav, R. Yadav, Protein modeling and active site binding mode interactions of myrosinase-sinigrin in *Brassica juncea* – an in silico approach, J. Mol. Graph. Model. 29 (2011) 740–746.
[17] S.F. Altschul, T.L. Madden, A.A. Schäffer, J. Zhang, Z. Zhang, W. Miller, D.J. Lipman, Gapped BLAST and PSI-BLAST: a new generation of protein database search programs, Nucleic Acids Res. 25 (1997) 3389–3402.
[18] N. Deshpande, K.J. Addess, W.F. Bluhm, J.C. Merino-Ott, W. Townsend-Merino, Q. Zhang, C. Knezevich, L. Xie, L. Chen, Z. Feng, R.K. Green, J.L. Flippen-Anderson, J. Westbrook, H.M. Berman, P.E. Bourne, The RCSB Protein Data Bank: a redesigned query system and relational database based on the mmCIF schema, Nucleic Acids Res. 33 (2005) 233–237.
[19] A. Sali, L. Potterton, F. Yuan, H. van Vlijmen, M. Karplus, Evaluation of comparative protein modeling by MODELLER, Proteins 23 (1995) 318–326.
[20] Discovery Studio Profile-3D User Guide, Biosym/MSI, San Diego, 2000.
[21] G.N. Ramachandran, C. Ramakrishnan, V. Sasisekharan, Stereochemistry of polypeptide chain configurations, J. Mol. Biol. 7 (1963) 95–99.
[22] V.Z. Spassov, P.K. Flook, L. Yan, LOOPER: a molecular mechanics-based algorithm for protein loop prediction, Protein. Eng. Des. Sel. 21 (2008) 91–100.
[23] R.A. Laskowski, D.S. Moss, J.M. Thornton, Main-chain bond lengths and bond angles in protein structures, J. Mol. Biol. 231 (1993) 1049–1067.
[24] M.J. Sippl, Recognition of errors in three-dimensional structures of proteins, Proteins 17 (1993) 355–362.
[25] R.E.B. Bernard, R. Brooks, B.D. Olafson, D.J. States, S. Swaminathan, M. Karplus, CHARMM: a program for macromolecular energy, minimization, and dynamics calculations, J. Comput. Chem. 4 (1983) 187–217.
[26] P. Aparoy, T. Leela, R.N. Reddy, P. Reddanna, Computational analysis of R and S isoforms of 12-lipoxygenases: homology modeling and docking studies, J. Mol. Graph. Model. 27 (2009) 744–750.
[27] A. Ohtaki, K. Murata, Y. Sato, K. Noguchi, H. Miyatake, N. Dohmae, K. Yamada, M. Yohda, M. Odaka, Structure and characterization of amidase from *Rhodococcus* sp. N-771: insight into the molecular mechanism of substrate recognition, Biochim. Biophys. Acta 1804 (2010) 184–192.
[28] C. Elisa, A. Sergio, Identification of the amino acid residues affecting the catalytic pocket of the *Sulfolobus solfataricus* signature amidase, Protein Pept. Lett. 17 (2010) 146–150.
[29] G. Wu, D.H. Robertson, C.L. Brooks, M. Vieth, Detailed analysis of grid-based molecular docking: a case study of CDOCKER-A CHARMm-based MD docking algorithm, J. Comput. Chem. 24 (2003) 1549–1562.
[30] Y.S. Zhao, K. Wang, H. Zeng, H.X. Zhang, J.H. Zhang, A comparative analysis of binding sites between human PKD1 and PKC1 based on homology modelling, molecular dynamics simulation and docking studies, Mol. Simul. 38 (2012) 309–314.